Concave Macrobicycles: Absorption Spectra, Luminescence Properties, and Endocavital Complexation of Neutral Organic Guests

Fritz Vögtle*[a], Ingo Michel[a], Ralf Berscheid[a], Martin Nieger[b], Kari Rissanen[c], Sirpa Kotila[c], Karri Airola[c], Nicola Armaroli[d], Mauro Maestri[d], and Vincenzo Balzani*[d]

Institut für Organische Chemie und Biochemie der Universität Bonn[a],
Gerhard-Domagk-Straße 1, D-53121 Bonn, Germany
Tel.: (internat.) +49(0)228-733495, Fax: +49(0)228-735662
E-mail: voegtle@snchemie1.chemie.uni-bonn.de

Institut für Anorganische Chemie der Universität Bonn[b],
Gerhard-Domagk-Straße 1, D-53121 Bonn, Germany

Department of Chemistry, University of Jyväskylä[c],
P.O. Box 35, FIN-40351 Jyväskylä, Finland

Dipartimento di Chimica "G. Ciamician", Università di Bologna[d],
Via Selmi 2, I-40126 Bologna, Italy

Received April 26, 1996

Key Words: Alkyne bridges / Charge transfer / Host compounds / Molecular cavities / Toposelectivity

By a mild modified Eglinton coupling a series of diyne-bridged macrobicyclic hosts capable of endocavital complexation were synthesized and their structures and complexation properties investigated by X-ray analysis. The inclusion of DMSO in **7** suggests a direct correlation between steric fit and orientation of the guest. On the basis of this hypothesis, the orientation of acetone in an endocavital inclusion of **2** was predicted and verified by X-ray analysis. Comparison of the single-crystal X-ray structures of the vacant macrobicycle **3** and of a family of macrobicycles showing endocavital or "pocket" complexation of neutral organic guests suggests that torsion of the cavities upon complexation results from induced fit. Hydrogenation of the triple bonds leads to the more flexible macrobicycles **10**–**12** with collapsable cavities. The absorption and emission spectra of the diyne-bridged macrobicyclic hosts **1** and **3**, of their hydrogenated analogues **11** and **12**, and of a hemicage parent compound of **2** (**14**) were investigated. The macrobicyclic compounds **3**, **11**, **12** and **14** exhibit a strong fluorescence in CH_2Cl_2 solution at room temperature. The lack of fluorescence of **2** under such conditions is attributed to the presence of low-energy charge-transfer excited states, as indicated by the charge-transfer bands in the absorption spectrum. In a rigid CH_2Cl_2 matrix at 77 K all the examined compounds are fluorescent.

One hundred years after Emil Fischer's "lock and key" hypothesis[1], many fundamental aspects of molecular recognition are not yet well understood. To enhance our knowledge in this field, investigation of tailored rigid molecular cavities is essential. In this paper we report on the synthesis, absorption and emission properties, and endocavital complexation of a series of new macrobicyclic hosts.

Hexa-2,4-diyne bridges in combination with aromatic spacers were earlier shown to provide cavities capable of housing organic guests[2]. By a mild, modified Eglinton coupling reported previously[3], some of us prepared several diyne-bridged concave macrobicycle hosts capable of complexing small neutral organic guests. The topology of the macrobicyclic cavities was determined by X-ray analysis and correlated with complexational and orientational selectivity. Hydrogenation of the alkyne bridges leads to more flexible macrobicycles which show a collapsed cavity in the solid state. The absorption and emission properties of diyne-bridged macrobicycles and their hydrogenated analogues were also investigated and interesting similarities and differences were revealed.

Results and Discussion

Syntheses and X-ray Structures

The macrobicycles **1**–**5** were synthesized by a mild, modified Eglinton coupling starting from the corresponding aromatic trispropargylethers (Scheme 1). Treatment of **1** with tetrafluoroborate in acetic anhydride yielded the dication **6**[3], which could be easily converted into the corresponding diol **7** by treatment with water in DMSO/dichloromethane[4] (Scheme 2).

The single crystal X-ray structure of **7** shows a cavity between the aromatic spacers held apart by rigid 2,4-hexadiyne bridges. As shown in Scheme 3, one molecule of DMSO is situated endocavitally, whereas two DMSO molecules and one ethanol molecule (not shown in Scheme 3 for the sake of clarity) are clathrate-bound. The DMSO guest molecule is located in the middle of the cavity with

0947–3440/96/1111–1697 $ 15.00+.25/0

Scheme 1. The diyne-bridged concave macrobicycles **1**–**5** were synthesized by a mild, modified Eglinton coupling in only two steps

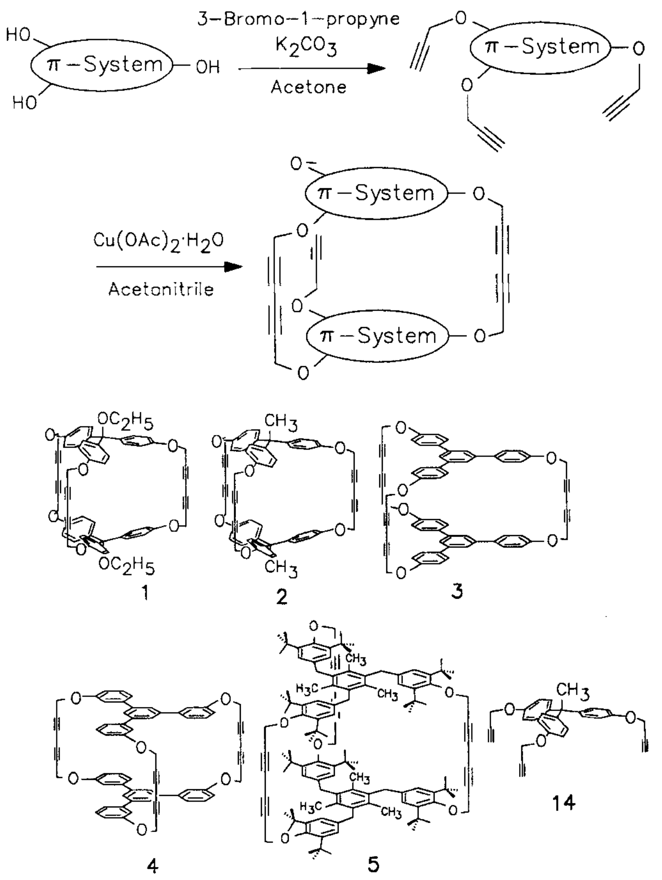

the oxygen atom lying near to the pseudo C_3 axis, only 70 pm from the center of gravity of the host. Short distances between the methyl groups of the guest and the aromatic rings of the host indicate multiple σ–π electronic interactions.

Scheme 2. The macrobicycle **7** was synthesized from **1** via the dication **6**[3]

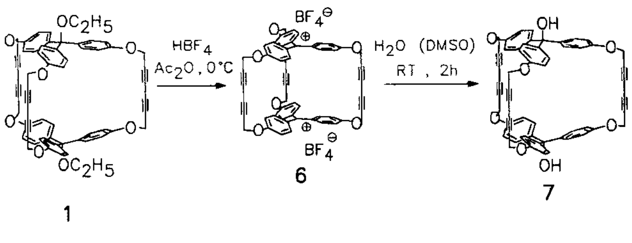

Hosts similar to the ones reported here are known to give complexes with benzene[5], phenylacetonitrile and acetonitrile[6]. In such cases, however, the guest is not placed in the center of the cavity, but more or less in a "window pocket" as shown by the view along the pseudo C_3 axis reported in Scheme 4. Only in the case of the inclusion of acetonitrile in **8** one half of the disordered guest is located in the center of the cavity.

The reason why **2** and **8** do not host their aromatic guests in the center of their cavity cannot be related to the size of their cavities, which according to X-ray analysis are big enough. But they are, similarly to that of **7**, approximately spherically shaped. The point is that flat aromatic guests are not sterically suitable for a spherically shaped host, so they just "stick" in a pocket built up by two aromatic rings of the spacers. Such a pocket, in contrast to the central cavity, provides a proper niche for σ–π interactions with aromatic guests which, as a consequence, do not show any tendency to be in the center of the cavity. The single-crystal X-ray structure of **7** suggests that guests like DMSO or acetone, with a more spherical orientation of the "binding sites", are more suitable for molecular inclusion by hosts with spherically shaped cavities. In order to check this interpretation we resynthesized the macrobicycle **2** and crystallized it from acetone. The single-crystal X-ray structure indeed showed inclusion of one acetone molecule whereas two others were clathrate-bound (Scheme 5). Acetone, like DMSO in **7**, is located right in the center of the cavity with the oxygen atom on the C_3 axis just 27 pm away from the center of gravity of the host. The "window" the guest's methyl groups are "pointing on" is 1045 pm, slightly larger than the two other windows (929 and 942 pm)[7].

Short distances between the methyl groups of the guest and the aromatic rings of the host indicate the presumed multiple σ–π interaction. The distance of H2'3 to the center of ring B is 300 pm and the angle CHAr is 170°. Even shorter distances are found between H3'2 and the centre of ring A (286 pm) and between H3'3 and the center of the bond between C16a and C17a (296 pm).

Flat aromatic spacers should be more suitable for complexation of flat aromatic guests[2]. Nevertheless, the single-crystal X-ray structure of **3** (Scheme 6) did not show any endocomplexation in the wide open cavity[8]. The distance of about 809 pm between the two spacers might be too large for efficient complexation of such guests by π–π interactions. (According to Whitlock and Whitlock[9], the ideal distance between two aromatic spacers for complexation of flat aromatic guests by π–π interactions is 684 pm.)

However, the vacant cavity of **3** shows a torsion along the pseudo C_3 axis of only about 2°. This is much less than in the above discussed structures which showed endo- or "pocket" complexation (Table 1). This might be an argument for an induced fit[10] caused by the complexation, as presumed earlier[5].

A larger spherically shaped cavity is achieved with **5**, which was synthesized in only two steps from Irganox® 1330, an industrial antioxidant[11]. The *t*-butyl groups not only improve solubility in organic solvents, but should also be replaceable, which could allow the preparation of tailored derivatives. MM$^+$ calculations[12] showed that in **5** the permanent cavity is partially occupied by the *t*-butyl groups, whereas in the de-*t*-butylated derivative of **9** a cavity suitable for larger guests is present. For example, a very good topological fit inside the electron-rich cavity of the latter compound was found for the spherically shaped, electron-poor C_{60} (Scheme 7).

Scheme 3. Single-crystal X-ray structure of the endocavital inclusion complex of **7** · DMSO and illustration of the shape and size of the cavity

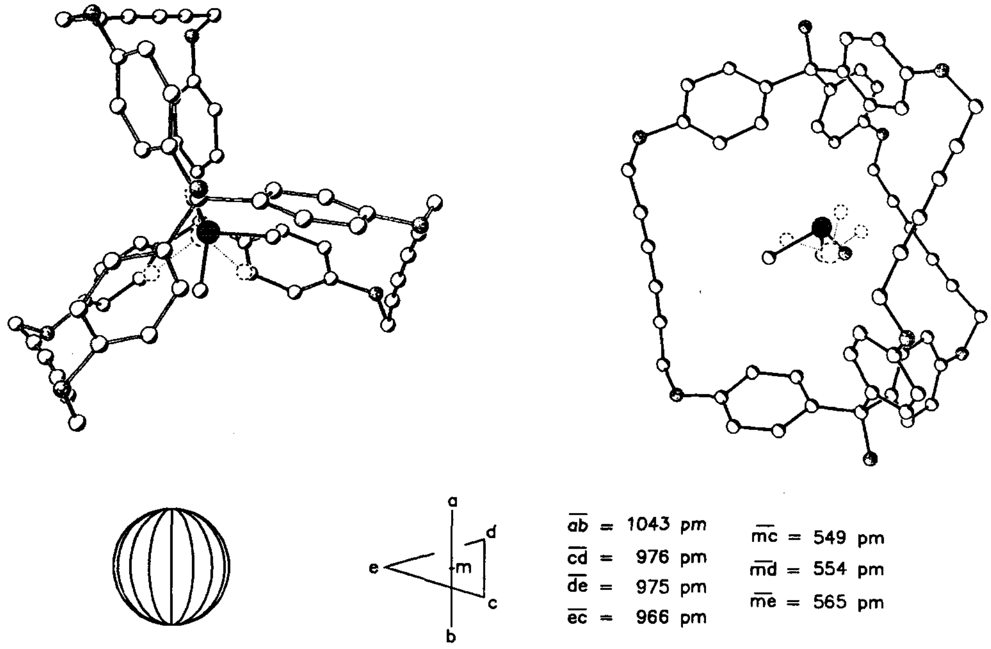

$\overline{ab}$ = 1043 pm
$\overline{cd}$ = 976 pm
$\overline{de}$ = 975 pm
$\overline{ec}$ = 966 pm
$\overline{mc}$ = 549 pm
$\overline{md}$ = 554 pm
$\overline{me}$ = 565 pm

7·DMSO

On this basis, the endocavital complexation of C_{60}, which might lead to a new method of topological purification, seems to be achievable in the near future.

More flexible potential hosts were obtained by hydrogenation of the macrobicycles **1**–**4** (Scheme 8). Treatment of the 2,4-hexadiyne-bridged macrobicyclic compounds **1**–**4** with hydrogen under palladium catalysis in toluene yielded the macrobicycles **10**–**13**. The structures of **10**, **11** and **12** were determined by single-crystal X-ray measurements. In all cases the crystal structure shows a "collapsed" cavity in the solid state. There are no indications of attractive interactions between the spacers. Thus due to their flexibility, the macrobicycles might be able to uptake neutral organic guests by an induced fit. In particular, the decrease of the spacer distance from 809 pm in **3** to about 500 pm in **12**, combined with the enhanced flexibility of the cage, should allow the nesting of guests with electron-poor double bonds inside the triphenylbenzene-spacered host.

Absorption and Luminescence Properties

A summary of the absorption and luminescence data is given in Table 2, where the data of **14**, the hemicage parent compound of **2**, are also shown for comparison purposes. The absorption and emission spectra of **14**, **2** and its hydrogenated analogue **11** in CH_2Cl_2 solution at room temperature are shown in Figure 1. In these compounds the prominent chromophoric component is methoxybenzene, which is known to exhibit an absorption band in the near UV region with a maximum at 277 nm[13]. The bands exhibited by **14**, **2** and **11**, in fact, are very similar to those of methoxybenzene. It can be noted, however, that the spectrum of **2** shows a shoulder around 260 nm and a tail above 300 nm. These spectral features are indicative of low-energy states which can be attributed to charge-transfer transitions from the electron donor[14] methoxybenzene units to the moderate electron acceptor[16] diyne units of the bridges. The presence of non-emitting, low-energy charge-transfer states in **2** is consistent with the lack of fluorescence at room temperature (Table 2, Figure 1).

In a rigid matrix at 77 K, where solvent repolarization cannot occur, the charge-transfer excited states are expected to move to high energy. Under such conditions, in fact, fluorescence of **2** can be observed. It is worth noticing that the hemicage compound **14** displays absorption and fluorescence properties very similar to those of **11**, without any evidence for low-energy charge-transfer excited states, in spite of the presence of methoxybenzene and diyne units. This seems to indicate that the cage structure of **2** offers the proper geometry and/or distance requirements for charge-transfer interactions.

The absorption and luminescence spectra of **3** and **12** are reported in Figure 2. In these compounds, methoxybenzene chromophoric units are still present but, in contrast to those in **2** and **11**, they are involved in an extended π-delocalized system through a central phenyl group. This leads (Table 2) to a dramatic increase in the molar absorption coefficient. It can also be noticed that the Stokes shift between absorption and emission maxima is much larger for **12** (10200 cm^{-1}) than for **11** (3400 cm^{-1}). Such a large Stokes shift, by analogy with biphenyl-type molecules[17], can be assigned to a decrease in the angle between the planes of the methoxybenzene unit and the central ring of the spacer in going from the ground to the excited state.

Scheme 4. Single-crystal X-ray structure of the endocavital inclusion complex of **8** · H_3CCN (above), **8** · BzlCN (middle) and **2** · 5 C_6H_6 (below) seen along the pseudo-C_3 axis and in the side view

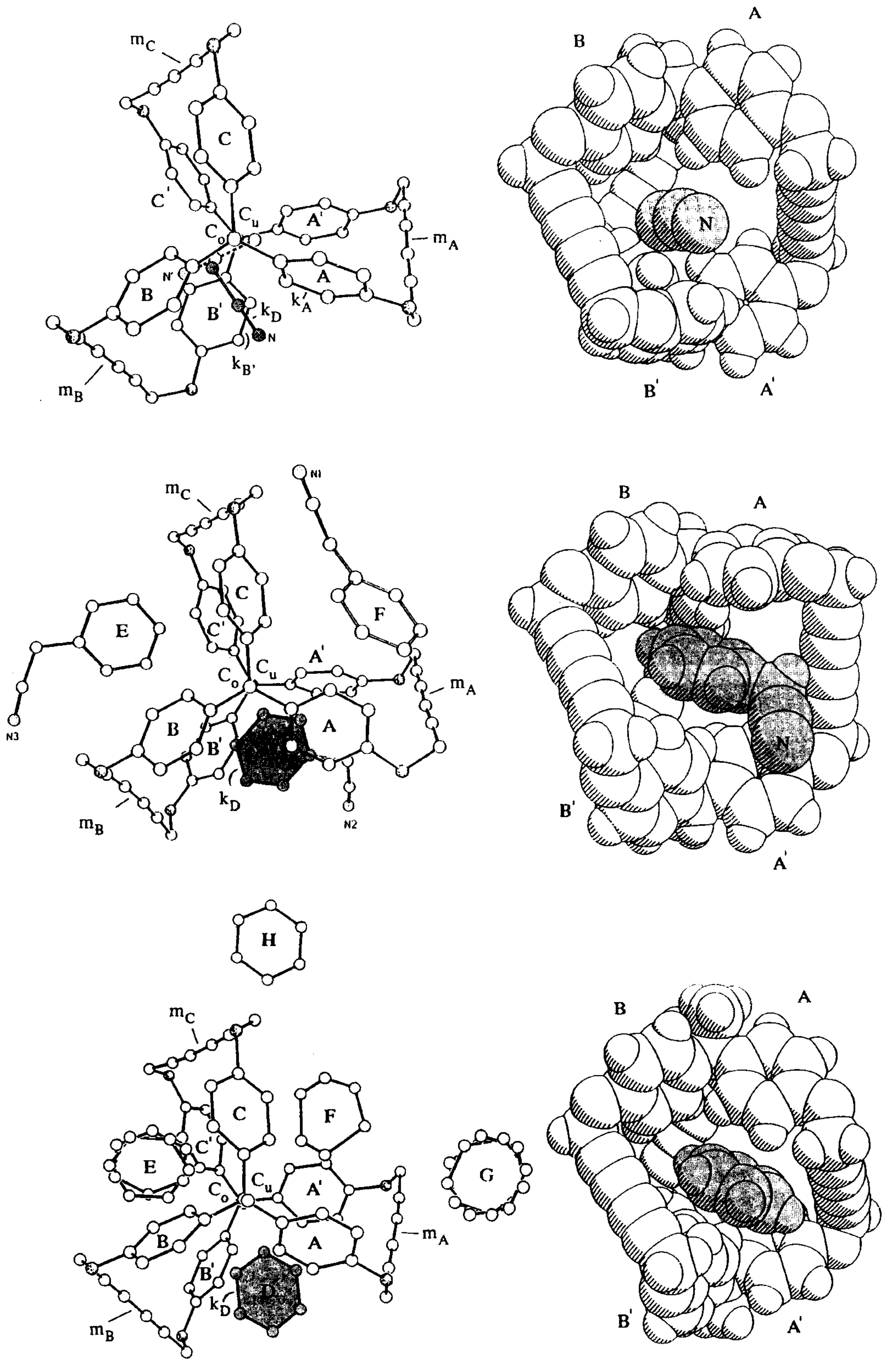

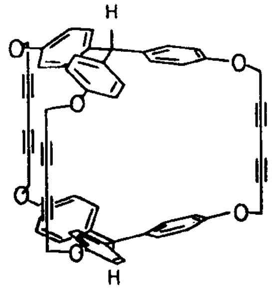

8

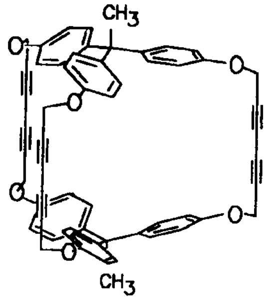

2

Compound **3** and its hydrogenated analogue **12** do not display strong differences in their absorption and luminescence properties, in contrast to the behavior of **2** and **11**. This indicates that the rigid structure of **3** prevents interaction between the methoxybenzene electron-donor groups and the diyne electron-acceptor groups.

Scheme 5. Single-crystal X-ray structure of the endocavital inclusion complex of **2** · acetone and illustration of the shape and size of the cavity

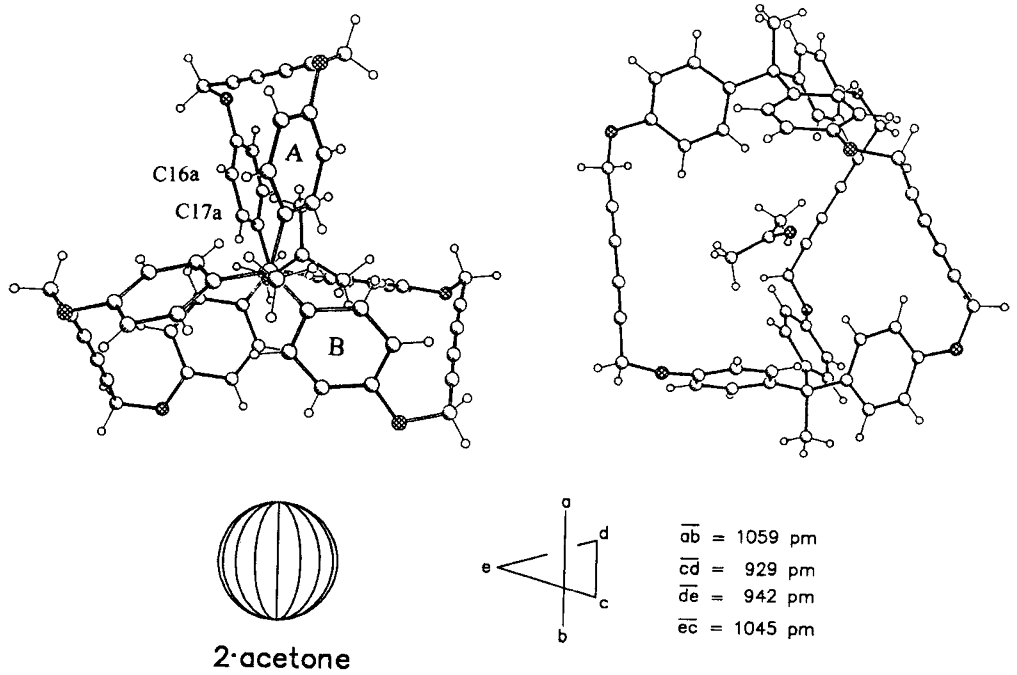

Scheme 6. Single-crystal X-ray structure of the concave macrobicycle **3** and illustration of the shape and size of the cavity

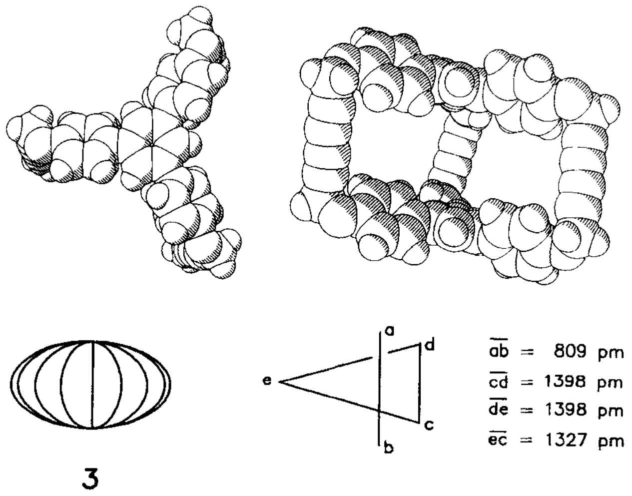

Scheme 7. Results of MM^+ calculations of the hypothetical macrobicycle **9** with an endocavital complexed C_{60}

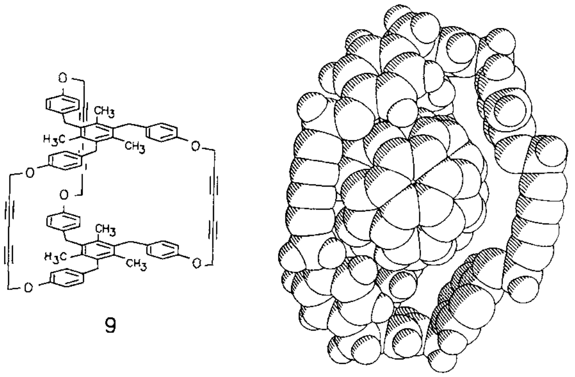

Table 1. Torsion along the pseudo C_3-axis

Compound	Torsion angle
7•DMSO	23°
3	2°
2•Me_2CO	35°
2•C_6H_6	35°
8•MeCN	36°
8•BzlCN	26°

Conclusions

Multiple bridging of aromatic spacers by rigid 2,4-hexadiynes leads to concave macropolycycles with permanent cavities capable of housing neutral organic guests. The guests are held inside the cage by multiple $\sigma-\pi$ interactions exclusively with the spacers. No interaction between guest and alkyne bridges was observed. On the other hand, intramolecular charge-transfer interactions between the aromatic spacers and the diyne bridges was observed for **2**. Such an interaction has a strong influence on the luminescence properties. As a general result, topological complementarity between the shape and "binding site" was shown to be essential for the location and orientation of the guests. With this strategy the synthesis of larger hosts with permanent spherically shaped cavities for the toposelective complexation of spherically shaped guests like C_{60} or small cryptands semms feasible. This might lead to improved solubility and transport rates of these species as well as to a new toposelective method as ternary complexes. Finally, it should be pointed out that the strong luminescence dis-

Scheme 8. Synthesis and single-crystal X-ray structures of the macrobicycles **10**–**13**

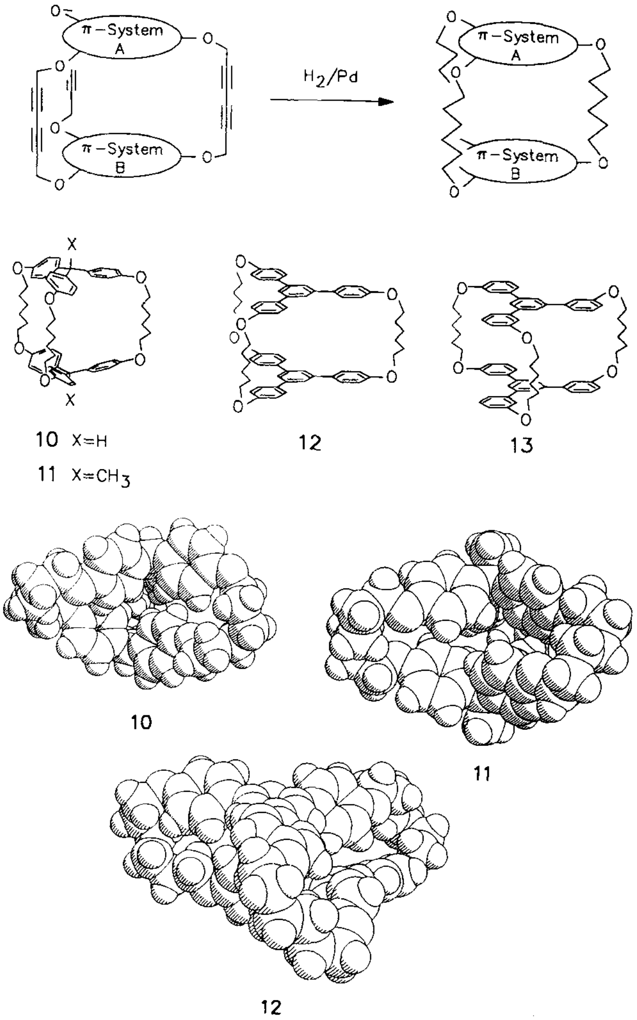

Table 2. Absorption and luminescence properties in CH_2Cl_2

	Absorption		Fluorescence				
			298 K			77 K	
	λ_{max} (nm)	ε (M^{-1} cm^{-1})	λ_{max} (nm)	τ[a] (ns)	Φ_{em}[b] (x 10^2)	λ_{max} (nm)	τ[a] (ns)
2	277	8700	—	—	—	294	4.1
11	279	9800	308	1.4	3.3	302	9.0
14	277	5000	306	1,2	1.9	304	5.0
3	265	70000	359	7.9	0.046	458	2.0
12	267	100.000	367	18.7	0.135	458	2.3

[a] Excited state lifetime. – [b] Luminescence quantum yield.

played by the aromatic spacers of these big host cages may be useful for the study of host–guest energy and electron-transfer processes[18], as recently shown for some hemicarceplexes[19].

Financial support from *NATO* and the *Italian MURST* is acknowledged. The *Academy of Finland* is thanked for granting a fellowship to S. K. and K. A. F. V. thanks the *Volkswagen-Stiftung* for financial support.

Figure 1. Absorption spectra (full lines) of compounds **2**, **11**, and **14** and fluorescence spectra (dashed lines) of compounds **11** and **14** in CH_2Cl_2 solution at room temperature. Compound **2** does not show any fluorescence under such conditions

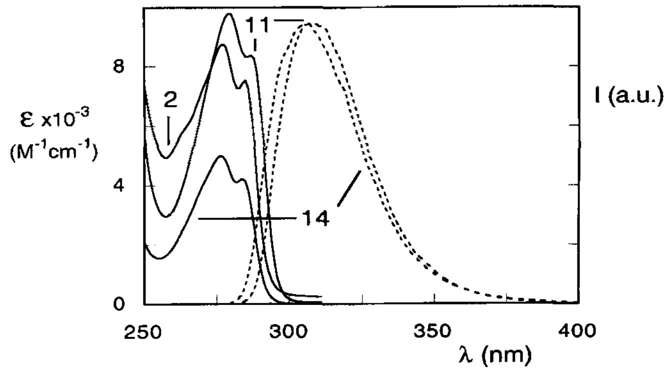

Figure 2. Absorption (full lines) and fluorescence (dashed lines) spectra of compounds **3** and **12** in CH_2Cl_2 solution at room temperature

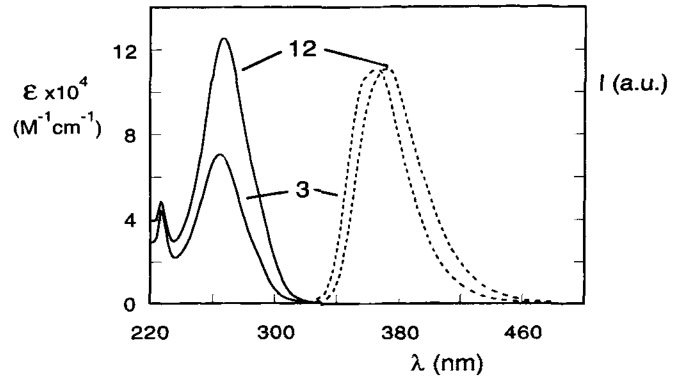

Experimental

General: ^1H and ^{13}C NMR: Bruker wm 250 (250 and 62.9 MHz respectively). – FAB-MS: Concept 1 H, Cratos, Manchester, GB, with *m*NBA as Matrix. – Melting points (uncorrected values): Tottoli melting-point apparatus SMP-20 (Büchi). – Thin-layer chromatography: TLC aluminum sheets, silica gel 60 F_{254} (Merck 5554).

Preparation of the Hexadiyne-Bridged Macrobicycles **3**, **4** *and* **5**.[20] – *General Procedure:* A suspension of 12.3 g (62 mmol) of $Cu(OAc) \cdot 2\,H_2O$ in 500 ml of acetonitrile was heated to 60 °C. Then a solution of 6.2 mmol of the corresponding trispropargylic ether in acetonitrile was added with stirring and the mixture was kept at 60 °C for 8 h. It was subsequently poured into 1 l of H_2O, the precipitate was filtered and washed with 500 ml of H_2O. The solid was dried in vacuo and purified by column chromatography.

8,15,29,36,47,54-Hexaoxadecacyclo[20.20.16.$2^{4,7}$.$2^{16,19}$.$2^{25,28}$.$2^{37,40}$.$2^{43,46}$.$2^{55,58}$.$1^{3,41}$.$1^{20,24}$]diaheptaconta1,3(59),4,6,16,18,20,22,24(64),25,27,37,39,41,43,45,55,57,60,62,65,67,69,71-tetradiacontaene-10,12,31,33,49,51-hexayne (**3**): Yield 10%; m.p. >250 °C, colorless powder; R_f (TLC, *n*-hexane/diethyl ether, 1:4; $SbCl_5$): 0.38 (brown). – ^1H NMR (400 MHz; $CDCl_3$): δ = 4.81 (s; 12 H; OCH_2), 7.0 (dd; ^3J = 8.6 Hz; ^4J = 2.5 Hz; 12 H; HC-2′–6′), 7.52 (dd; ^3J = 8.6 Hz; ^4J = 2.5 Hz; 12 H; HC-3′–5′), 7.55 (s; 6 H; ar. H). – ^{13}C NMR (100.6 MHz; $CDCl_3$): δ = 55.45 (6 CH_2; OCH_2), 71.26 (6 C; C≡C), 74.45 (6 C; CH_2C≡), 114.91 (12 CH; C-2′, -6′), 124.21 (6 CH; C-2), 128.56 (12 CH; C-3′, -5′), 134.68 (6 C; C-1), 141.90 (6 C, C-1′), 156.55 (6 C; C-4′). – FAB-MS: ($C_{66}H_{42}O_6$): *m*/*z* = 931.3 ([M^+]).

9,16,32,39,59-Hexaoxadecacyclo[22.22.18.1^{4,8}.1^{17,21}.1^{22,26}.1^{27,31}.1^{40,44}.1^{3,45}.1^{47,51}.1^{60,64}]diaheptacontal,3(65),4,6,8(66),17,19,21(67),22,24,26(68),27,29,31(69),40,42,44(70),45,47,49,51(71),60,62,64(72)-tetradiacontaen-11,13,34,36,54,56-hexayne (**4**): Yield 8%; m.p. >250 °C, colorless powder; R_f (TLC, *n*-hexane/diethyl ether, 1:4; $SbCl_5$): 0.49 (brown). – ^1H NMR (250 MHz; $CDCl_3$): δ = 5.08 (s; 6H; OCH_2), 5.12 (s; 4H; OCH_2), 6.96–7.07 (m; ^3J = 7.7 Hz, ^4J = 1.9 Hz; 3H; HC-4′), 7.42–7.54 (m; 4H), 7.43 (t; ^3J = 7.7 Hz; 3H; HC-5′), 7.61 (s; 2H; HC-2), 7.85 (s; 1H), 8.0 (s; 2H). – ^{13}C NMR (62.9 MHz; $CDCl_3$): δ = 56.0/56.8 (6 CH_2; O-CH_2), 73.3/75.8 (6 C; C≡C), 76.4/78.6 (6 C; CH_2*C*≡), 113.0 (3 CH; C-2′), 113.9/114.4 (3 CH; C-4′), 117.6 (3 CH; C-6′), 124.5 (3 CH; C-2), 130.1/130.2 (3 CH; C-5′), 141.6/141.7 (2 × 3 C; C-1, -1′), 157.6, 157.9 (3 C; C-3′). – FAB-MS ($C_{66}H_{42}O_6$): *m/z* = 931.2 ($[M]^+$).

7,18,30,41,50,61,67,68,72,73,76,77-Dodeca-tert-butyl-2,23,25,46,65,70-hexamethyl-9,16,32,39,52,59-hexaoxadecacyclo-[22.22.18.2^{5,7}.2^{17,20}.2^{28,31}.2^{40,43}.2^{48,51}.2^{60,63}.1^{3,45}.1^{22,26}]octaheptacontal-1,3(65),5,7,17,19,22,24,26(70),28,30,40,42,45,48,50,60,62,66,68,71,73,75,77-tetradiacontaene-11,13,34,36,54,56hexayne (**5**): Yield 17%; m.p. >285 °C, colorless powder; R_f (TLC, *n*-hexane/diethyl ether, 1:4; $SbCl_5$): 0.80 (red). – ^1H NMR (250 MHz, $CDCl_3$): δ = 1.29 (s; 108H; $C(CH_3)_3$), 2.36 (s; 18H; CH_3), 4.04 (s; 12H; $ArCH_2Ar$), 4.44 (s; 12H; OCH_2), 6.92 (s; 12H; Ar-H). – ^{13}C NMR (62.9 MHz; $CDCl_3$): δ = 17.42 (6 CH_3; $ArCH_3$), 32.22 (36 CH_3; $C(CH_3)_3$), 35.70 (12 C; $C(CH_3)_3$), 35.77 (6 CH_2; $ArCH_2Ar$), 63.99 (6 CH_2; OCH_2), 71.20 (6 C; ≡*C*CH_2), 75.63 (6 C; ≡C−C≡), 126.60 (12 CH; C-2′, -6′), 133.76/134.80/136.28 (3 × 6 C; C-1, -2, -1′), 143.40 (12 C; C-3′, -5′), 155.11 (6 C; C-4′). – FAB MS ($C_{126}H_{162}O_6$): *m/z* = 1771.4 ($[M + H]^+$).

Preparation of the Hexane-Bridged Macrobicycles **10**, **11**, **12** *and* **13**. – *General Procedure:* To a solution of 0.2 mmol of the corresponding hexadiyne-bridged macrobicycle in 100 ml of toluene, 160 mg of 10% palladium on carbon (equivalent to 0.08 mmol of palladium) was added. The suspension was shaken at 3 bar hydrogen for 8 h and the catalyst was removed by filtration through a short filter column. After evaporation of the solvent the product was purified by column chromatography.

out,out-6,13,23,30,39,46-Hexaoxaoctacyclo[16.16.16.2^{2,5}.2^{14,17}.2^{19,22}.2^{35,38}.2^{42,50}]dohexaconta-2,4,14,16,19,21,31,33,35,37,47,49,51,53,55,57,59,61-octadecaene (**10**): Yield 70%; m.p. 172 °C, colorless powder; R_f (TLC, *n*-hexane/diethyl ether, 1:4; $SbCl_5$): 0.57 (red). – ^1H NMR (250 MHz; $CDCl_3$): δ = 1.54 (s; 12H; CH_2), 1.76 (br. t; ^3J = 5.6 Hz; 12H; CH_2), 3.95 (t; ^3J = 5.6 Hz; 12H; CH_2), 5.36 (s; 2H; $HCAr_3$), 6.71 (d; ^3J = 8.7 Hz; 12H; HC-3, -5), 6.96 (d; ^3J = 8.7 Hz; 12H; HC-2, -6). – ^{13}C NMR (62.9 MHz; $CDCl_3$): δ = 24.21 (6 CH_2; CH_2), 28.04 (6 CH_2; CH_2), 54.50 (2 C; Ar_3C), 66.99 (6 CH_2; CH_2 a), 114.51 (12 CH; C-3, -5), 129.98 (12 CH; C-2, -6), 136.82 (6 C; C-1), 157.57 (6 C; C-4). – FAB-MS ($C_{56}H_{62}O_6$): *m/z* = 831.4 ($[M + H]^+$).

out,out-1,18-Dimethyl-6,13,23,30,39,46-hexaoxaoctacyclo-[16.16.16.2^{2,5}.2^{14,17}.2^{19,22}.2^{35,38}.2^{42,50}]dohexaconta-2,4,14,16,19,

Table 3. Crystallographic data and summary of data collection and refinement

Compound	2	7	10	11	12
formula	$C_{58}H_{42}O_6$ ·3 acetone	$C_{56}H_{38}O_8$ ·3 DMSO·2 x 0.5 ethanol	$C_{56}H_{62}O_6$	$C_{58}H_{66}O_6$	$C_{66}H_{66}O_6$ ·0.5 toluene
crystal size	0.10 x 0.30 x 0.35	0.20 x 0.25 x 0.35	0.20 x 0.25 x 0.40	0.30 x 0.40 x 0.50	0.15 x 0.20 x 0.43
crystal system	monoclinic	monoclinic	triclinic	trigonal	triclinic
space group	P2_1/c (no. 14)	C2/c (no. 15)	P $\bar{1}$ (no. 2)	R $\bar{3}$ c (no. 167)	P $\bar{1}$ (no. 2)
a, Å	14.420 (1)	42.473 (11)	11.316 (2)	14.014 (1)	9.294 (1)
b, Å	31.360 (2)	13.299 (2)	13.000 (1)	14.014 (1)	24.261 (3)
c, Å	12.645 (1)	29.371 (4)	16.517(2)	43.771 (3)	25.385 (4)
α, deg	90	90	94.42 (1)	90	99.98 (1)
β, deg	91.48 (1)	133.71 (1)	105.60 (1)	90	90.29 (1)
γ, deg	90	90	99.94 (1)	120	98.93 (1)
V, Å^3	5716.4 (6)	11992 (5)	2285.5 (5)	7444.9 (7)	5566 (1)
Z	4	8	2	6	4
ρ (calc), g cm^{-3}	1.173	1.240	1.208	1.150	1.195
μ, mm^{-1}	0.616	1.625	0.604	0.571	0.583
F(000)	2136	4720	892	2772	2140
diffractometer			Enraf Nonius CAD4		
radiation			CuK		
λ, Å	1.54178	1.54178	1.54178	1.54178	1.54178
T [K]	293	293	200	293	293
max 2Θ, deg	120	130	110	120	104
no. of unique data	8463	9753	5335	1237	12364
full-matrix least-squares refinement	F^2	F^2	F^2	F^2	F^2
on no. of variables/restraints	649/24	808/80	578/99	99/0	1483/830
R[for I > 2σ(I)]	0.089	0.099	0.071	0.045	0.083
wR2	0.334	0.308	0.204	0.139	0.322

21,31,33,35,37,47,49,51,53,55,57,59,61-octadecaene (**11**): Yield 70%; m.p. 262°C, colorless powder; R_f (TLC, *n*-hexane/diethyl ether, 1:4; $SbCl_5$): 0.63 (mauve). – ^1H NMR (250 MHz; $CDCl_3$): δ = 1.53 (br. s; 12H; CH_2), 1.83 (br. t; ^3J = 6 Hz; 12H; CH_2), 2.10 (s; 6H; CH_3), 3.96 (t; ^3J = 6 Hz; 12H; CH_2), 6.72 (d; ^3J = 8.8 Hz; 12H; HC-3, -5), 6.92 (d; ^3J = 8.8 Hz; 12H; HC-2, -6). – ^{13}C NMR (62.9 MHz; $CDCl_3$): δ = 24.87 (6 CH_2; CH_2 a), 28.24 (6 CH_2; CH_2 b), 30.19 (2 CH_3), 50.59 (2 C; Ar_3C); 67.43 (6 CH_2; CH_2 a), 113.85 (12 CH; C-3, -5), 129.56 (12 CH; C-2, -6), 141.81 (6 C; C-1), 157.16 (6 C; C-4). – FAB-MS ($C_{58}H_{66}O_6$): *m/z* = 859.5 ([M + H]$^+$).

8,15,29,36,47,54-Hexaoxadecacyclo[20.20.16.2^{4,7}*.2*^{16,19}*.2*^{25,28}*.2*^{37,40}*.2*^{43,46}*.2*^{55,58}*.1*^{3,41}*.1*^{20,24}*]diaheptaconta-1,3(59),4,6,16,18,20,22,24(64),25,27,37,39,41,43,45,55,57,60,62,65,67,69,71-tetradiacontaene* (**12**): Yield 63%; m.p. 252°C, colorless powder; R_f (TLC, *n*-hexane/diethyl ether, 1:4; $SbCl_5$): 0.56 (blue-green). – ^1H NMR (250 MHz; $CDCl_3$): δ = 1.59 (br. s; 12H; CH_2), 1.80 (br. t; ^3J = 5.8 Hz; 12H; CH_2), 3.96 (t; ^3J = 5.8 Hz; 12H; CH_2), 6.69 (d; ^3J = 6.8 Hz; 12H; HC-3′, -5′), 7.21 (d; ^3J = 6.8 Hz; HC-2′, -6′), 7.27 (s; 6H, HC-2). – ^{13}C NMR (62.9 MHz; $CDCl_3$): δ = 23.11 (6 CH_2; C-c), 28.20 (6 CH_2; C-b), 66.24 (6 CH_2; C-a), 114.60 (12 CH; C-2′, -6′), 123.22 (6 CH; C-2), 128.04 (12 CH; C-3′, -5′), 133.53 (6 C; C-1), 141.29 (6 C; C-1′), 158.40 (6 C; C-4′). – FAB-MS ($C_{66}H_{66}O_6$): *m/z* = 954.5 ([M]$^+$).

9,16,32,39,59-Hexaoxadecacyclo[22.22.18.1^{4,8}*.1*^{17,21}*.1*^{22,26}*.1*^{27,31}*.1*^{40,44}*.1*^{3,45}*.1*^{47,51}*.1*^{60,64}*]diaheptaconta-1,3(65),4,6,8(66),17,19,21(67),22,24,26(68),27,29,31(69),40,42,44(70),45,47,49,51(71),60,62,64(72)tetradiacontaene* (**13**): Yield 70%; R_f (TLC, *n*-hexane/diethyl ether, 1:4; $SbCl_5$): 0.77 (green-yellow). – ^1H NMR (250 MHz; $CDCl_3$): δ = 1.54–1.65 (br. m; 12H; CH_2), 1.96–2.04 (br. m; ^3J = 5.8 Hz; 12H; CH_2), 4.06 (t; ^3J = 6.4 Hz; 6H; CH_2), 4.27 (t; ^3J = 7.6 Hz; 6H; CH_2), 6.90–6.94 (m; 6H; HC-5′), 7.23–7.38 (m; 18H; ar. H), 7.80–7.83 (m; 6H; HC-4′). – MS ($C_{66}H_{66}O_6$): *m/z* = 954.4 ([M]$^+$).

X-ray Crystallographic Studies: The structures were solved by direct methods (SHELXTL-plus). Non-hydrogen atoms were refined anisotropically; hydrogen atoms were refined using a riding model (SHEL-93). An extinction correction was applied to **7**, **11**, and **12**. An absorption correction on the basis of scans was applied to **2** and **12** and by use of DIFABS to **7**. Disorder was found for the hexano bridges in **10** and **12** and for the solvent in **7** and **12**. Details of the data collection and refinement are compiled in Table 3.

An X-ray structure analysis of **3** was carried out, but the nature of the included solvent could not be determined. Only the conformation of the macrobicycle is well-defined [crystal data: space group *Pbcn* (no. 60), *a* = 22.827(1), *b* = 16.226(1), *c* = 18.355(1) Å, *V* = 6799(1) Å^3, *Z* = 4].

Absorption and Luminescence Spectra: Absorption spectra were measured with a Perkin-Elmer λ6 spectrophotometer, emission spectra were recorded with a Perkin-Elmer LS50 spectrofluorimeter equipped with a Hamamatsu R-928 photomultiplier; emission quantum yields were determined using the method of Demas and Crosby[20]. Excited-state lifetimes were measured with an Edinburgh Instruments 199 Single Photon Counting System (D_2 lamp). Uvasol Merck dichloromethane was used as solvent.

---

[1] [1a] E. Fischer, *Ber. Dtsch. Chem. Ges.* **1894**, *27*, 2985. – [1b] J.-M. Lehn, *Supramolecular Chemistry*, VCH, Weinheim (Germany), **1995**. – [1c] F. Vögtle, *Supramolecular Chemistry*, Wiley, Chichester (U. K), **1991**, **1993**.

[2] [2a] E. T. Jarvi, H. W. Whitlock Jr., *J. Chem. Soc.* **1980**, *102*, 657; B. P. Friederichsen. – [2b] H. W. Whitlock Jr., *ibid.* **1989**, *111*, 9132.

[3] [3a] R. Berscheid, M. Nieger, F. Vögtle, *Chem. Ber.* **1992**, *125*, 2539. – [3b] R. Berscheid, F. Vögtle, *Synthesis* **1992**, 58.

[4] R. Berscheid, *Dissertation*, University of Bonn, **1992**.

[5] D. O'Krongly, S. R. Denemeade, M. Y. Chiang, R. Breslow, *J. Am. Chem. Soc.* **1985**, *107*, 5544.

[6] [6a] F. Vögtle, R. Berscheid, W. Schnick, *J. Chem. Soc., Chem. Commun.* **1991**, 414. – [6b] R. Berscheid, M. Nieger, F. Vögtle, *Chem. Ber.* **1992**, *125*, 1687.

[7] The size of the window is taken as the distance between centers of the diyne bridges.

[8] The R-value of the single-crystal X-ray structure of **3** is 0.19 due to the not determined nature of the included solvent.

[9] B. J. Whitlock, H. W. Whitlock, *J. Am. Chem. Soc.* **1994**, *116*, 2301.

[10] D. E. Koshland Jr., *Angew. Chem.* **1994**, *106*, 2468; *Angew. Chem. Int. Ed. Engl.* **1994**, *33*, 2375.

[11] We are grateful to the CIBA GEIGY AG and Dr. *H.-R. Meier* for providing us with a sample of IRGANOX® 1330.

[12] Computer-generated space-filling model (molecular geometry by force field calculations) Molek 9000: P. Bischof, ISKA, D-Bensheim **1992**; HP-9000/825 SRX; MM$^+$; Autodesk HyperChem ™2.0 **1992**; N. L. Allinger, *J. Am. Chem. Soc.* **1977**, *99*, 8127.

[13] H. H. Jaffé, M. Orchin, *Theory and Applications of Ultraviolet Spectroscopy*, Wiley, New York, **1962**.

[14] The oxidation potential of methoxybenzene is +1.79 V (vs. SCE)[15].

[15] C. K. Mann, K. K. Barnes, *Electrochemical Reactions in Nonaqueous Systems*, M. Dekker ed., New York, **1970**.

[16] The reduction potential of *p*-methoxydiphenylacetylene is −2.24 V (vs. SCE)[15].

[17] I. B. Berlmann, *Handbook of Fluorescence Spectra of Aromatic Molecules*, Academic Press, London, **1965**.

[18] V. Balzani and F. Scandola, *Supramolecular Photochemistry*, Horwood, Chichester, **1991**.

[19] [19a] D. J. Cram, *Nature* **1992**, *356*, 29. – [19b] A. J. Parola, F. Pina, M. Maestri, N. Armaroli,R. Ballardini, V. Balzani, *New J. Chem.* **1994**, *18*, 559. – [19c] F. Pina, A. J. Parola, E. Ferreira, M. Maestri, N. Armaroli, R. Ballardini, V. Balzani, *J. Phys. Chem.* **1995**, *99*, 12701. – [19d] A. Farràn, K. Deshayes, C. Matthews, I. Balanescu, *J. Am. Chem. Soc.* **1995**, *117*, 9614.

[20] The macrobicyclic compounds **3**–**5** and **10**–**13** showed strong absorption (clathration) of solvent which was not completely removable by high vacuum. The diyne-bridged macrobicycles could not be analyzed by EI, but only by FAB-MS which did not allow high resolution measurement.

[21] Further details of the crystal structure investigations may be obtained from the Fachinformationszentrum Karlsruhe, D-76344 Eggenstein-Leopoldshafen (FRG) on quoting the depository numbers CDS-405 530 (**7**), CDS-405 531 (**11**), CDS-405 532 (**10**), CDS-405 533 (**2**) and CDS-405 534 (**12**).

[22] J. N. Demas, G. A. Crosby, *J. Phys. Chem.* **1971**, *75*, 991.

[96113]